Spatially hierarchical nano-architecture for real time detection of Interleukin-8 cancer biomarker

Sawsen Azzouzi, Mounir Ben Ali, Francesca Bellagambi, Abdelhamid Elaïssari, Nicole Jaffrezic-Renault, Abdelhamid Errachid, Nadia Zine

Version of Record: https://www.sciencedirect.com/science/article/pii/S0039914022002326
Manuscript_a81441cfef581e59f41c0127db215595

Spatially hierarchical nano-architecture for real time detection of Interleukin-8 cancer biomarker

Sawsen Azzouzi[a], Mounir Ben Ali[a], Francesca Bellagambi[b], Abdelhamid Elaissari[b], Nicole Jaffrezic-Renault[b], Abdelhamid Errachid[b,*], Nadia Zine[b]

[a] University of Sousse, Higher Institute of Applied Sciences and Technology of Sousse, GREENS-ISSAT, Cité Ettafala, 4003 IbnKhaldoun Sousse, TUNISIA
[b] University of Lyon 1, Institut des Sciences Analytiques (ISA) – UMR 5280, 69100 Villeurbanne, Lyon, FRANCE

[*]Corresponding author: Prof. Abdelhamid Errachid
E-mail address: abdelhamid.errachid-el-salhi@univ-lyon1.fr
Telephone: +33 43 74 23 560
Scopus Author iD: 6602163740

Abstract

In the present work we have developed two hierarchical nano-architectures based electrochemical immunosensors for the detection of interleukin-8 (IL-8) cytokine tumor biomarker. A comparative study has been performed for spatial nano-architectures and their relative sensing to establish the model for real time monitoring. With the first platform, the recognition layer consisted with immobilised IL-8 on aminothiol modified gold electrodes. In the second approach, the activated multi walled carbon nanotubes (MWCNT-COOH) were added in the functionalisation process by covalent attachment between the functionalities NH_2 of aminothiol and the functionalities COOH of carbon nanotubes. The surface topology of the recognition layer has been characterised by atomic force spectroscopy (AFM) and contact angle (CA) measurements. The electrochemical response of the developed sensor was measured by electrochemical impedance spectroscopy (EIS). A side-by-side comparison showed that aminothiol/activated MWCNTs/ anti-IL-8 based impedimetric immunosensor exhibits high reproducibility (The relative standard deviation (R.S.D) = 3.2 %, n = 3) with high stability. The present sensor allows evaluating a lower detection limit of 0.1 pg mL^{-1} with a large dynamic sensitivity range from 1 pg $mL^{-1}$to 1000 pg mL^{-1} covering the entire clinical therapeutic window. The developed MWCNTs based immunosensor has been calibrated by determining IL-8 in artificial plasma and showed a selective response to IL-8 even in the interfering environment of other cytokines such as Interleukin-1 (IL-1) and Interleukin-6 (IL-6).

Keywords: Spatially Hierarchical nano-architecture; Immunosensor; Multi wall carbon nanotubes (MWCNT); Impedance spectroscopy; Interleukin-8; Cancer biomarker.

1. Introduction

Early diagnosis of cancer is very important for successful diagnostic of the disease and patient survival and makes a challenge and critical step for cancer therapy. In fact, it needs accurate detection of a certain protein biomarkers present trace amount in serum patients of early stages of cancer disease [1,2,3]. The present traditional assay methods are radio-immunoassay and enzyme-linked immunosorbent assay (ELISA) [4], immune-polymerase chain reaction (PCR) assay [5], electrophoretic immunoassay [6], fluorescence immunoassay [4], and mass spectrometric immunoassay [7]. Most of these existing methods need expensive, sophisticated instruments and well-controlled experimental conditions. Moreover, ELISA tests are time-consuming with time-to-results of several hours and are limited in their applicability for Point-of-Care (PoC) devices. Subsequently, there is a great interest for developing biosensors for protein detection with a faster and highly sensitive and selective immunological response [8,9] that leads to reduced costs of treatment with a fundamental understanding of disease progression. In this context, during the last years, immunosensors were widely used in order to enhance the biosensors metrological characteristics. These devices combine an antibody as recognition element with a transducer, which converts optical, electrical, and mass changes of the solution into a measurable signal following the interaction between the free antigen (Ag) present in the solution under analysis and the antibody (Ab) anchored to a transducer. Another advantage of biosensors compared to traditional methods for detecting IL-8 is they can already be integrated in PoC devices, which are well known to allow faster medical decisions, to avoid any trouble related to specimen identification and sample transport problems, and the needing only small sample volumes [9].

Interleukin 8 (IL-8) is a bioactive protein produced by many different cells of the immune system [10]. It is a 8 kDa cytokine that is involved in the inflammatory response with serum levels in healthy individuals at ≤13 pg mL^{-1} compared to 20–1000 pg mL^{-1} or more in cancer patients [11,12]. Increased concentrations of IL-8 have found in the presence of many types of cancer [13], including squamous cell cancer [11], prostate cell carcinoma[14], thyroid cancers [12], and pancreatic cancer [15], implying a great clinical interest in the quantification of IL-8 cytokines for both cancer prognosis and diagnosis [16,17]. Recent research has addressed the detection and monitoring of IL-8 by biosensing approaches. For instance, Otieno *et al.* [18] have incorporated an on-line chamber to capture cancer biomarker proteins on magnetic beads derivatised with 300,000 enzyme labels and 40,000 antibodies into a modular microfluidic immunoarray. Domnanich *et al* [19] presented a reflective gold chips coated with polyelectrolyte multilayers for signal enhancement in immunoassays for melanoma-relevant

biomarkers. A technique for reversibly encapsulating nanomechanical resonant sensors within microfluidic channels for the detection of IL-8 in fetal bovine serum was also described by Waggonera *et al*. [20]. Malhotra et al. combined gold nanoparticles surfaces with magnetic beads massively labelled with horseradish peroxidase enzyme labels to develop an ultrasensitive electrochemical microfluidic array optimized to measure a four-protein panel of cancer biomarker proteins [21]. Mandal *et al*. presented an optofluidic biosensor platform for the concurrent detection of multiple interleukins (IL-4, IL-6, and IL-8), by incorporating a unique one-dimensional photonic crystal resonator array that enables light-matter interaction [22]. Hakim et al; have fabricated polysilicon nanowire based biosensors using a top-down process in order to quantify the binding constant of two inflammatory biomarkers: IL-8 and TNF-α (tumor necrosis factor-alpha) [23]. Hakim et al. integrated an enzymatic signal enhancement scheme onto a multiplexable silicon photonic microring resonator platform for the detection of IL-8, IL-2 and IL-6 [24]. More recently, other biosensing methods have been proposed for detecting blood IL-8 at ever-lower levels through the optimization and continuous progresses of electrochemical detection strategies as well as the use of nanostructured surfaces. In 2016, Sharma *et al*. [25] proposed a free-label biosensor based on electrochemical impedance spectroscopy (EIS) that exploited a novel synthetic non-antibody capture protein based on a cystatin scaffold, managing to reach a sub-pg/mL sensitivity. Low limits of detection of pg mL^{-1} were achieved also by Tonello *et al*. in 2016 [26], by testing commercially-available carbon sensors modified using two different carbon nanostructures (e.g. Carbon nanotubes and spherical fullerene) in combination with stripping voltammetry, and by Verbarg et al. in 2017 through the implementation of an optical detection platform combined with a fluorescent immunoassay [27].

It is therefore clear that electrochemical bio-chemical sensors coupled with functionalising process using nanostructured materials can be considered as a good strategy to improve the biosensing development. Moreover, further progresses can be achieved by the use of EIS, which is undoubtedly acknowledged as a powerful tool for interfacial characterization. EIS is a sensitive technique that monitors the electrical response of the studied system after application of a periodic small amplitude signal. This technique is a direct method for probing protein binding events such as those from antibody-antigen interactions [28].

Due to their electrical, optical, thermal, and mechanical properties, carbon nanotubes (CNT) were widely used in the functionalisation of electrodes in order to amplify electrical signals of the chemical and biological sensors, with an increasing number of applications of CNTs in several chemical analysis fields [29,30]. The enhancement of CNTs electrode kinetics to

different redox species, in terms of increased faradic current and minimisation of the redox overpotential, has made the nanotubes to be considered as electrocatalytical materials. Thus, the electronic properties of CNTs and specially their band structure, in terms of density of electronic states, are of great interest for the interfacial electron transfer between a redox system in solution and the electrode surface [29–31].

This work presents two different functionalisation techniques for the development of an EIS biosensor for the detection of IL-8. The first functionalisation approach consisted in immobilising activated IL-8 antibodies on 11-amino-1-undecanethiol modified gold electrodes in order to create a two-dimensional nano-architecture . The second strategy provided that , activated multi walled carbon nanotubes (MWCNT-COOH) were added in the functionalisation process by covalent attachment between the functionalities NH_2 of aminothiol and the functionalities COOH of carbon nanotubes. That lead to develop a three-dimensional spatially hierarchical nano-architecture which offers a larger active specific area in contact with the analyte to enhance the immunosensor performances.

2. Materials and Methods

2.1 Reagents

Multi-Walled Carbon Nanotubes (MWCNT-COOH) (ref DRP-CNT sol), were provided by DROPSENS (Spain).11-amino-1-undecanthiol was obtained from Sigma Aldrich. N-(3-dimethylaminopropyl)-N-ethyl-carbodiimide hydrochloride (EDC), N-hydroxysuccinidmide (NHS) and sodium dodecyl sulfate salt (SDS), used as surfactant was provided by Sigma–Aldrich (France). Anti-human IL-8 monoclonal antibody (anti IL-8), Recombinant Human IL-8, Recombinant Human IL-6 and Recombinant Human IL-1 were all purchased from R&D Systems (France). The bicinchoninic acid protein assay (BCA protein assay) kit was provided by Pierce (France). The buffer solution used for all experiments was Phosphate Buffer Saline (PBS; pH=7.4). All solutions were made up in ultrapure water produced by a Millipore Milli-Q system. Artificial plasma was purchased from Biolabo (France).

2.2 Instrumentation and experimental details

The different layers grafted onto the gold electrode were characterised by contact angle measurements using a Dataphysics, Contact Angle System OCA (France). The measurements were analyzed with a droplet of 4 µL of deionized water, for the untreated gold substrate and after each stage of the gold substrate treatment. The contact angle has been obtained in three

different areas of the given wafer with three separated drops and we have calculated the statistical validation of the three measurements.

The surface topology of aminothiol/ activated MWCNTs functionalised gold substrates were investigated using Atomic Force Microscopy (AFM). The AFM measurements were performed in 'tapping-mode' (TM-AFM) and the respective images were recorded at room temperature with a Nano- Observer AFM microscope from SCIEN Tec (France).

The UNICO Spectrophotometer Model S-2150 UV-Vis (Spain) was used for the colorimetric quantification of the amount of anti IL-8 immobilised on the working electrode surface.

Cyclic Voltammetry (CV) and electrochemical impedance spectroscopy (EIS) were performed in a conventional electrochemical cell containing a three-electrode system using a VMP3 potentiostat/galvanostat (Bio-logic-Science Instrumentation, France). A reference electrode (Ag/AgCl) and platinum (Pt) counter electrode wire with a diameter of ~0.5 mm were used. CV measurements were performed in a mixture of 5 mM $K_3[Fe(CN)_6]/K_4[Fe(CN)_6]$ as the redox probe in PBS solution (pH 7.4). The potential was swept between -200 mV and 600 mV (versus Ag/AgCl) at a rate of 100 mV/s. Impedance measurements were carried out in the same solution at room temperature. A sinusoidal excitation signal with amplitude of 10 mV was applied and the impedance spectra were recorded in the frequency range (0.1 Hz - 100 kHz).The potential polarization was optimized at - 220 mV. The obtained EIS data were fitted by the EcLab software. All electrochemical measurements were performed inside a Faraday cage.

2.3 Antibodies and cytokines preparation

Antibodies and cytokines were diluted in PBS buffer, aliquoted, and stored at −20 °C following the supplier's protocol. The used cytokines IL-8, IL-1 and IL-6 were aliquoted at varying concentrations ranging from 1 to 1000 pg mL^{-1} and stored at 4 °C.

2.4 Gold electrodes fabrication

The microelectronics fabrication process for the gold electrodes has been performed at Centro Nacional de Microelectronica CNM (Barcelone, Spain). The starting material is P-type〈100〉 silicon 100 mm diameter wafers with a nominal thickness of 525 μm. The process starts with a dray oxidation process to grow a layer of SiO_2 (780Å) and afterward a Si_3N_4 layer of 1000 Å thickness was deposited by low-pressure chemical vapor deposition (LPCVD). For a better adhesion of Au microelectrodes, a 100 Å of Ti layer was introduced first, and then the 2500 Å

of Au layer was sputtered onto the surface. After, the wafer had been diced into individual chips with size about 1 cm^2.

2.4.1. Gold electrode modification with 11-amino-1-undecanethiol self-assembled monolayer

Before functionalisation, the gold electrode was cleaned in an ultrasonic bath for 15 min in acetone and dried under a N_2 flow. Subsequently, the gold electrode was dipped for 3 min at room temperature in a piranha solution, and then rinsed with ultrapure water. Subsequently, working gold electrode was immersed in 1 mM 11-amino-1-undecanethiol (aminothiol) solution for 5 h at 4 °C, in order to create an amine layer over the gold support. The substrate was then rinsed with ethanol to remove the unbonded thiols. It is well known that the formation of a self-assembled monolayer (SAM) provided functional groups for subsequent covalent attachment by carbodiimide method to form peptide bonds. In particular, the use of 1-ethyl-3-(3-dimethylaminopropyl)carbodiimide (EDC), which is currently one of the most used the hetero-crosslinker for covalent antibody immobilization, provides a stable bond between a carboxyl group and a primary amine. Hydrophilic residues with chemically reactive functionalities (e.g. amino, carboxyl, and hydroxyl groups) are generally at the antibody surface, and the EDC/NHS coupling of antibody amine and carboxyl groups to surface carboxyl and amine groups represents one of the most used strategies for oriented antibody immobilization [32]. Moreover, the use of 11-amino-1-undecanethiol proven to provide NH_2 terminated SAM with a higher antigen/antibody ratio than a COOH terminated SAM [33].

2.5. Preparation of the immunosensors

2.5.1. Preparation of aminothiol / activated anti IL-8 based immunosensor (Platform 1)

The carboxyl groups present in the terminal part of the anti IL-8 antibody (10 μg mL^{-1}) were activated by reaction with 0.2 M NHS and 0.8 M EDC prepared in PBS buffer, for 45 min. The modified anti IL-8 structures were then added to the Au-NH_2 layer for 1h at room temperature (Fig. 1A). Subsequently, the biosensor was incubated into 1% ethanolamine for 20 min, to deactivate unreacted –COOH groups, which could eventually lead to non-specific bonds during IL-8 detection stage [9].

2.5.2. Preparation of aminothiol / activated MWCNTs / anti IL-8 based immunosensor (Platform 2)

Before immobilising the carbon nanotubes on aminothiol functionalised gold electrodes, 17 μL from 0.25 mg/mL MWCNT were dispersed in 183 μL of deionised H_2O containing 0.1 M

sodium dodecyl sulphate (SDS). This produces a final volume of 200 µL of MWCNT–COOH mixture. Then, 0.2 M solution of NHS and 0.8 M solution of EDC were prepared in PBS in order to produce a final volume of 200 µL. Afterwards, 200 µL of MWCNT solution and 200 µL of NHS/EDC solution were mixed for 45 min in order to formulate the active EDC/NHS ester groups on the MWCNTs. Finally, the aminothiol modified working electrode was incubated in MWCNT/NHS/EDC solution for 2 h at room temperature, and followed this by rinsing in PBS to remove all non-bound MWCNTs. This produces a 0.011 mg mL^{-1} concentration of functionalized MWCNTs [34]. The active NHS ester functionalised carbon nanotubes MWCNT-COOH attached on gold electrodes were then maintained in contact with 10 µg mL^{-1} ofanti IL-8 antibody for 1 h at room temperature (Fig. 2A) to react with the terminal amino groups of the antibody as already described by []. The excess antibodies were removed by rinsing with PBS. As done for Platform 1, the IL-8 antibody-modified gold electrode was treated with 1% ethanolamine solution for 20 min to deactivate unreacted –COOH groups from MWCNT,. Finally, the substrate was rinsed with PBS.

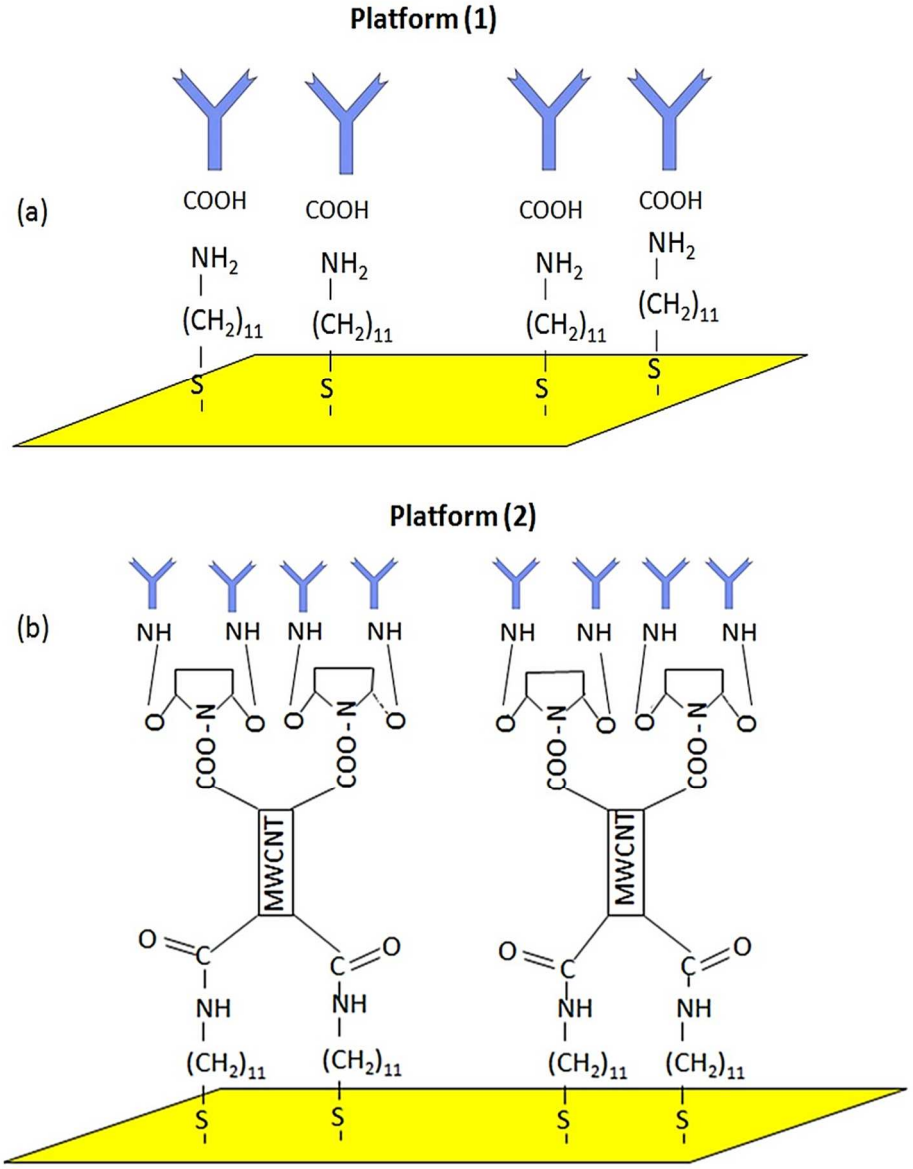

Fig. 1. Schematic presentation of the main steps for biofunctionalisation process of the developed immunosensors: **(A)** Anti-IL-8 antibody activation and its subsequent immobilization onto the Au-NH_2 layer; **(B)** Immobilization of carbon MWCNT on aminothiol functionalised gold electrodes through the activation of MWCNT by using NHS/EDC, followed by anti-IL-8 antibody binding.

2.5.3. Antibody / antigen affinity reaction

All procedures were made in triplicate. The antigen solution with increasing concentrations, prepared in PBS buffer (pH=7.4) by accurate dilution of a 5 µg/mL stock solution, was incubated on the bio-functionalised surface for 30 min at room temperature.

3. Results and discussion

3.1 Morphological characterisation of the functionalised gold electrode

Contact angle (CA) measurements were made to characterise the different functionalisation steps of the gold electrode. The contact angle was 81 ± 2° for the bare gold electrode, in agreement with the expected angle of 81 ± 1° [36], whilst, the gold electrode treated with piranha was 53 ± 2°. This hydrophilic character proves the presence of COOH as the terminal group. The modification of gold electrode with aminothiol leads to the decrease of the CA to 26 ± 2°. This signifies that the aminothiol was successfully self-assembled on the gold electrode. In fact, the thiol function -SH leads to the spontaneous formation of a strong Au-sulphur interaction that is expected to form a closely packed monolayer [37]. Subsequently, the immobilisation of the activated MWCNTs leads to a remarkable increase in the contact angle (74°± 1°). This reflects the hydrophobic character of carbon nanotubes. Finally, the decrease of the contact angle to 62°± 2° shows the successful immobilisation process of IL-8 antibodies. Images obtained from CA measurements are shown in Fig. 1S (Supplementary material section).

The AFM images of aminothiol functionalised gold electrode after MWCNTs and IL-8 antibodies immobilisation are presented in Fig. 2.

Fig. 2A shows round pores corresponding to gold surface. A dispersion of nano-objects is observed with an average diameter of 30-35 nm and a surface roughness (RMS) of 9.34 nm which proves the successful immobilisation of carbon nanotubes as MWCNTs bundles. The length of MWCNT bundles is not observable due to the interaction of the tip with surface [38,39]. Then, the presence of the IL-8 antibodies on the gold/aminothiol/ MWCNTs based structure was evident from the significant change observed in the surface roughness with a RMS=3.56 nm (Fig. 2B).The observed surface was also quite uniform, suggesting that most of the antibodies had a similar orientation after binding.

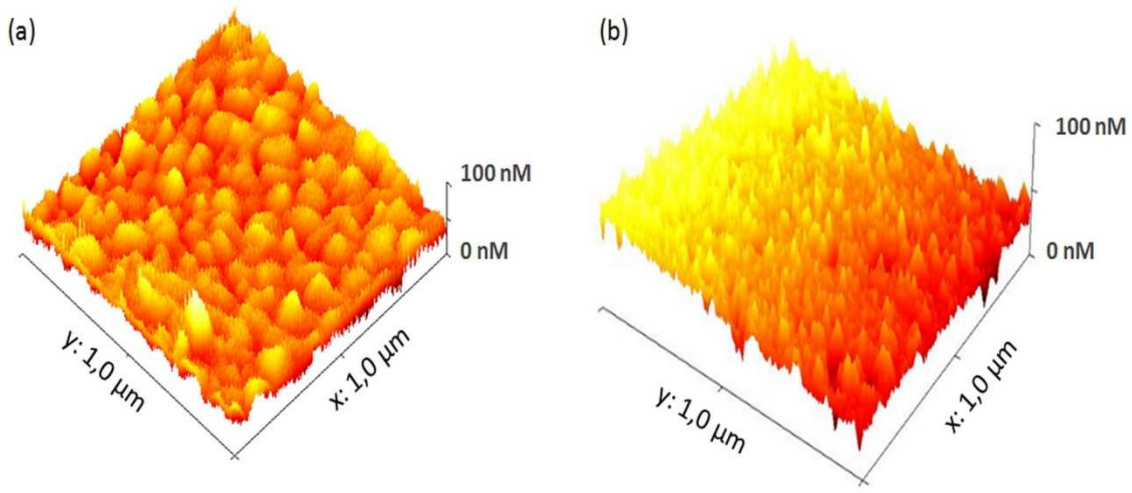

Fig. 2. AFM image of aminothiol modified gold electrode after **(A)** MWCNTs and **(B)** IL-8 antibodies immobilization.

3.2 Electrochemical characterisation of aminothiol SAMs

The compactness and the blocking effect of SAMs modified electrode has been investigated using CV through a redox behavior of a reversible Fe $(CN)_6^{3-}$ /$Fe(CN)_6^{4-}$ pair [40–42]. Fig. 3 illustrates the cyclic voltammograms before and after functionalisation of gold electrodes with aminothiol. The oxidation and reduction peaks the bare electrode were recorded at ~ 0.301 V and 0.155 V. However, the redox peaks decreased after the formation of SAMs onto the working gold electrode. This was attributed to the SAMs acting as an insulating layer that blocked the electron transfer at the electrode interface.

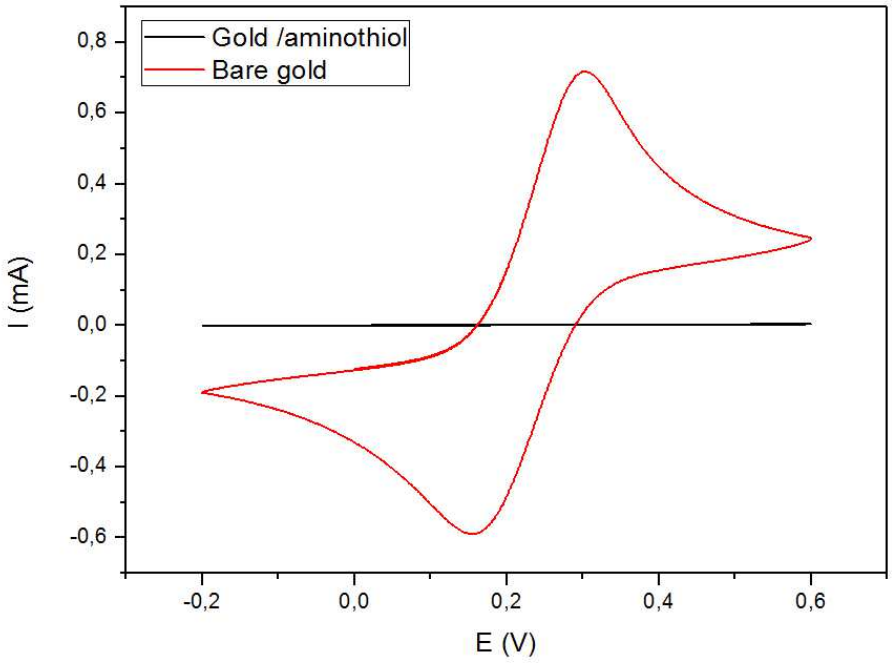

Fig. 3. Cyclic voltammograms for bare gold and aminothiol modified electrode in 5 mM $K_3[Fe(CN)_6]/K_4[Fe(CN)_6]$ in PBS (pH=7.4). The scan rate was 100 mV/s.

3.3 Electrical characterisation of the biofilm by impedance spectroscopy

EIS was performed to control the building-up of the biofilms based on aminothiol and aminothiol / MWCNTs structures at an optimised potential of −220 mV. This value was set since it allowed minimizing total impedance of the modified electrode before IL-8 addition [43]. Fig. 4 shows the Nyquist diagrams for the assembly of the biofilms on the working gold electrode. We notice for the first system, the presence of activated IL-8 antibodies attached to the aminothiol layer was confirmed by a decrease of the charge transfer resistance (R_{ct}) which measures directly the ability of the charge transfer to take place between electrodes and surrounding electrolyte.

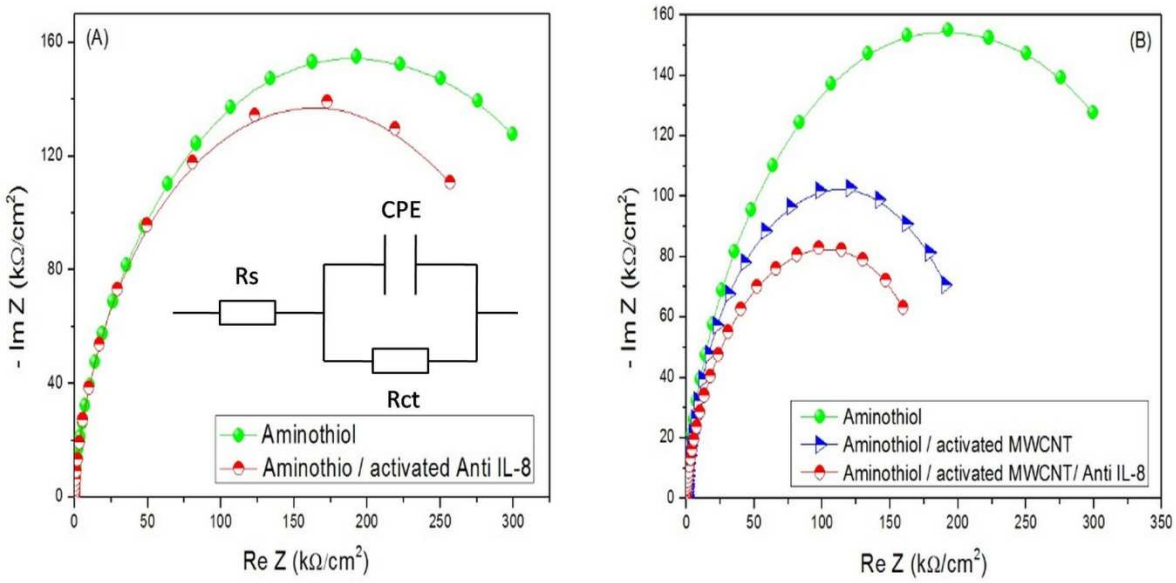

Fig. 4. Nyquist diagram for the impedance measurements (at -0.22 V) vs. Ag/AgCl in PBS solution (pH 7.4) corresponding to the various layers grafted onto the gold electrode. Spectra were obtained between 0.1 Hz – 100 kHz; amplitude of alternative voltage 10 mV.

With the MWCNTs based platform, we can observe a significant decrease of the interfacial impedance after carbon nanotubes immobilisation that reflects the attachment of the carbon nanotubes on aminothiol and brings out their conducting properties. In fact, the MWCNTs layer promotes the electron transfer through the layer of thiol and increases the conductivity of the system, and therefore the charge transfer rate. Then, the immobilisation of IL-8 antibodies leads to the decrease of the interfacial impedance. This can be attributed to the increase of MWCNTs conductance.

3.4 Determination of the total concentration of anti IL-8 being modified onto the working electrodes

The BCA Protein Assay, which is a biochemical assay commonly used for quantitation of total protein in a sample, was used in order to quantify the IL-8 antibodies concentration by measuring the net absorbance at 562 nm using a UV-visible spectrophotometer. This assay combines the reduction of Cu^{2+} to Cu^{1+} by protein in an alkaline medium with the highly sensitive and selective colorimetric detection of the cuprous cation (Cu^{1+}) by bicinchoninic acid. First, solutions of anti IL-8 with known concentrations have been prepared and used as samples, and analysed by using the BCA protein assay in order to construct the standard curve. The tubes containing the standard solutions and the working reagents were covered and

incubated at 60°C for 30 min. Then, after cooling all the tubes to room temperature, the absorbance (A562 nm) of all the samples was measured within 10 minutes.

The second step consists in incubating the anti IL-8 modified gold working electrodes with unknown immobilised protein concentration using the same protocol and measuring the absorbance at 562 nm and finally quantifying the unknown concentration using the standard calibration curve. The measured concentrations of anti IL-8 were 1.3 ± 0.1 µg/mL (R.S.D = 7.6 %; n = 3) and 22.1 ± 1.2 µg/mL (R.S.D = 5.4 %; n=3) for aminothiol based immunosensor (platform 1) and MWCNTs based three-dimensional nanoarchitecture (platform 2), respectively.

Table 1 summarizes the measured concentrations of anti IL-8 attached to the surface for both studied platforms. We can notice that the measured concentration of anti IL-8 was higher in the case of MWCNTs based immunosensor (22.1 ± 1.2 µg/mL). This could be due to the three-dimensional (3D) structure of MWCNTs based nano-architecture that offers a larger specific surface area and subsequently more available recognition sites in contact with the analyte.

Table 1. Total concentration of anti IL-8 immobilized onto the electrode.

Structure	Concentration of anti IL-8 immobilized onto the electrode (µg/mL)	RSD (%; n=3)
Aminothiol / activated anti IL-8	1.3 ± 0.1	7.6
Aminothiol / activated MWCNTs / anti IL-8	22.1 ± 1.2	5.4

3.5 Impedimetric response of the immunosensors

Before the immobilisation of the antibody, the biosensors were tested by addition of antigen (IL-8), no change in the impedance spectrum was observed for both platforms. Then, the anti IL-8 functionalised gold electrode was calibrated in presence of increasing concentrations of the specific antigen IL-8 ranging from 1 pg mL^{-1} to 1000 pg mL^{-1}. Antigen–antibody interactions were monitored using impedance spectroscopy. The impedance spectra obtained after addition of increasing concentrations of antigen (IL-8) are shown as Nyquist plots, in Fig. 5A and 5B, where Re Z is the real part and −Im Z is the imaginary part of the complex impedance Z. A semicircle plot can be observed that is characteristic of a pure resistance in parallel with a capacitance [43].

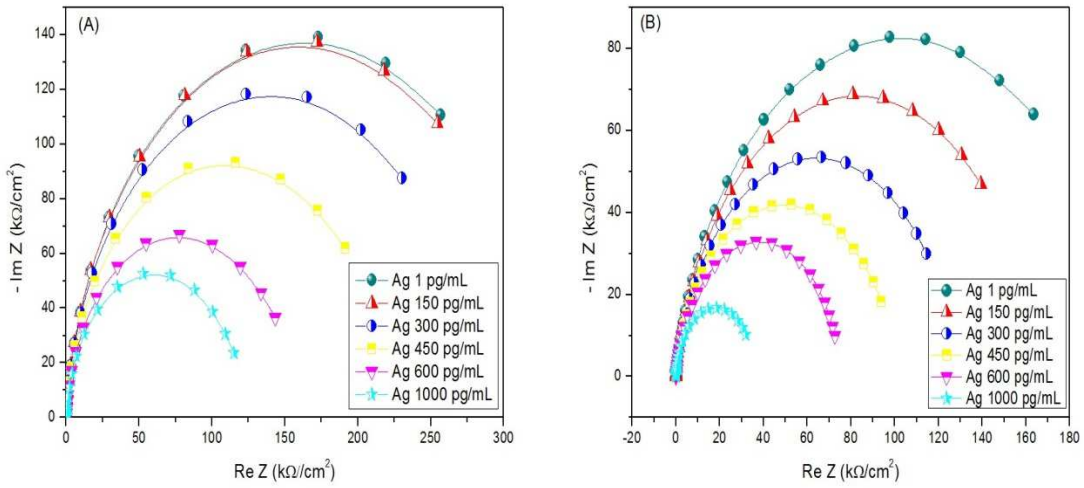

Fig. 5. Examples of Nyquist plots obtained at -0.22 V vs. Ag/AgCl in PBS performing EIS measurements on (A) aminothiol / anti IL-8 modified gold electrode (B) aminothiol/ MWCNT/ anti IL-8 under various concentrations of IL-8 antigen (pH 7.4, Spectra were obtained between 0.1 Hz – 100 kHz. Amplitude of Alternative voltage: 10 mV).

As it can be seen from Fig. 5, at low frequencies, the half-cercles diameter decreases clearly with the increase of IL-8 concentration for both immunosensors. This can be due to the decrease in the electron transfer resistance reflecting the interaction between the IL-8 antigen and the bio-functionalised surface. For, the MWCNTs based nano-architecture, the increase of MWCNTs conductivity could be explained by the increase of the negative charge of the immunocomplexe [39].

From an electrochemical point of view, a Randles equivalent circuit can represent the solid/electrolyte interface. In such model, the Warburg impedance Z_w attributed to the mass transfer to the electrode surface, is in series with the charge transfer resistance R_{ct} and both are generally in parallel with a double layer capacitance C_{dl}. R_s resistance added in series represents the resistance of the electrolyte. However, In this work, Z_w is almost small and remains negligible compared with the resistance of the charge transfer R_{ct} at the biofunctionalised gold electrode / electrolyte interface. Subsequently, the impedance spectra were fitted with the equivalent circuit, shown as inset in Fig. 4A. It consists of a charge transfer resistance R_{ct} in parallel with a constant phase element CPE. A resistance R_s was added in series with them.

The constant phase element CPE reflects the inhomogeneities and defect areas of the layer [45]. In fact, it is a capacitance reflecting the non-ideality of the double-layer at the bio-

functionalised gold electrode/electrolyte interface due to the roughness and porosity of the biofilm and can be expressed as follows:

$$Z_{CPE} = \frac{1}{Q\,(j\omega)^{n}}$$

Where Q is a constant, j is the imaginary number, ω is the angular frequency and $0 < n < 1$. CPE becomes more capacitive, when the value n tends to 1.

The different simulated fitting parameters from the impedance data obtained for the increasing IL-8 concentration are summarised in Table 1 and Table 2.

Table 2. Fitting parameters obtained for the aminothiol/activated anti IL-8 based immunosensor.

IL-8 Concentration	Rs (Ω)	CPE1 (µF)	n	R_{ct1} (kΩ)	χ^2 (10^{-3})
1 pg mL^{-1}	552 ± 2	1.635 ± 0.005	0.919 ± 0.005	314 ± 1	0.194
150 pg mL^{-1}	564 ± 1	1.778 ± 0.002	0.919 ± 0.006	309 ± 1	0.192
300 pg mL^{-1}	587 ± 3	1.726 ± 0.003	0.911 ± 0.008	265 ± 2	0.205
450 pg mL^{-1}	552 ± 2	1.798 ± 0.001	0.929 ± 0.005	210 ± 3	0.400
600 pg mL^{-1}	538 ± 2	1.825 ± 0.006	0.939 ± 0.003	150 ± 3	0.527
1000 pg mL^{-1}	531 ± 3	1.875 ± 0.005	0.938 ± 0.009	116 ± 3	0.542

Table 3. Fitting parameters obtained for the aminothiol/activated MWCNTs/anti IL-8 based immunosensor.

IL-8 Concentration	Rs (kΩ)	CPE2 (µF)	n	R_{ct2} (kΩ)	χ^2 (10^{-3})
1 pg mL^{-1}	2 ± 0.1	2.798 ± 0.003	0.969 ± 0.001	202 ± 1	0.457
150 pg mL^{-1}	2 ± 0.1	2.799 ± 0.001	0.969 ±0.004	167 ± 1	0.393
300 pg mL^{-1}	2 ± 0.1	2.800 ± 0.001	0.971 ± 0.007	128 ± 1	0.132
450 pg mL^{-1}	2 ± 0.1	2.789 ± 0.005	0.959 ± 0.003	97 ± 0.5	0.100
600 pg mL^{-1}	2 ± 0.1	2.801 ± 0.007	0.959 ± 0.009	77 ± 0.3	0.159
1000 pg mL^{-1}	2 ± 0.1	2.799 ± 0.004	0.968 ± 0.001	35 ± 0.3	0.309

CPE1 and CPE2 values are not affected by the increase of the IL-8 concentration and remains constant. However, the resistance of the charge transfer R_{ct1} and R_{ct2} were found to be the

most sensitive to the changes in IL-8 concentration and were, thus, selected as the relevant parameters to monitor the sensitivity of both developed immunosensors. The MWCNT based immunosensor is more sensitive promoting of the electron transfer thanks to carbon nanotubes properties and their particularity to amplify the response signal from antibody–antigen interaction and to improve the immunosensors characteristics. In fact, the MWCNTs facilitate the electron transfer between the electroactive species and the electrodes and facile oxidation and reduction kinetics [46]. Thus, , the calibration curves for both systems corresponding to the variation of the charge transfer resistance R_{ct} *vs* IL-8 concentrations were realised in order to quantify the biosensors response, and they could be find in Fig. 2S (Supplementary material section).

The immunosensors calibration curves present a linear relationship between the resistance of the charge transfer and the IL-8 concentration ranging from 150 pg mL^{-1} to 600 pg mL^{-1} (R^2 = 0.9961) with a detection limit of 100 pg mL^{-1} for the aminothiol based two-dimensional (2D) platform and from 1 pg mL^{-1} to 1000 pg mL^{-1} (R^2 = 0.9969) with a lower limit of detection of 0.1 pg mL^{-1} for the MWCNTs based immunosensor, covering the entire clinically interesting range of IL-8 concentrations, which is very important not only for the early-stage diagnosis and screening procedures, but also in mapping the stage of the cancer too. Comparing both spatially hierarchical nano-architectures, we can notice that the use of MWCNT-COOH modified gold electrodes leads to a lower detection limit and a higher saturation limit with an extended linear range against IL-8 concentration [36]. This can be due to the higher concentration of immobilised anti IL-8 (22 ± 1 µg mL^{-1}) due to the three-dimensional (3D) structure of MWCNTs based nano-architecture that offers a larger specific surface area. Moreover, the MWCNTs play a dual amplification role in both the recognition and transduction events. In addition, we can notice that the use of EIS provides a direct method of Antibody–Antigen binding and offers fast, sensitive, selective and quantitative responses [47–49]. Therefore, the impedimetric MWCNTs based three-dimensional immunosensor was selected for further evaluation of selectivity and possible application.

The reproducibility of both impedimetric immunosensors was investigated by repeated experiments (n = 3). A relative standard deviation of 7 % was obtained for the first system based on aminothiol and of 3 % for the MWCNTs based three-dimensional platform. The response of the developed impedimetric immunosensors was almost completely stable for one month.

3.6 Selectivity

Another important parameters related to the analytical performances of MWCNTs based three-dimensional immunosensor is its specificity and selectivity. Therefore, the ability of the biosensor to discriminate IL-8 from foreign species was investigated by evaluating the signal responses of the developed immunosensor to IL-8 against two other interfering compounds. This study was applied to Interleukin-1 (IL-1) and Interleukin-6 (IL-6). The selected non-specific antigen (IL-1 and IL-6) have been also demonstrated to be overexpressed in the presence of different cancers [50,51]. In general, the observed selectivity will depend mostly on the selectivity/specificity of the Ab/Ag reaction and of the non-specific response presented by the immunosensor platform. At the same concentration, the signal produced by the biosensor in the presence of the target analyte (IL-8) was always higher by at least 3 orders of magnitude compared to that observable by analyzing possible interferents (IL-1 and IL-6). A clear increase in signal was observed in presence of IL-8. In contrast, no significant signal was observed for IL-1 and IL-6 even at high concentration level of 1000 pg $mL^{-1}$and consequently, we did not observe significant influence during the detection of IL-8 when mixed IL-1 and IL-6. This result confirmed the higher affinity of IL-8 and brings out the specific and selective properties of the developed MWCNTs based immunosensor. The average R_{ct} changes produced by the addition of 1 pg mL^{-1} IL-8, 1000 pg mL^{-1} IL-1 and 1000 pg mL^{-1} IL-6 are presented in Fig. 3S (Supplementary materials section).

3.7 Test in commercialised artificial plasma

The goal of the present work was the development of a spatially hierarchical nano-architecture based electrochemical immunosensor for real time detection, in human samples, of IL-8, that can be considered as early warning marker for cancer disease. Thus, the suitability of the developed MWCNT based immunosensor for the detection of IL-8 in real sample was investigated by testing the impedimetric signal response in artificial plasma. So, in order to reduce the non-specific adsorption, the artificial plasma was diluted 1000 times and has been used to prepare the solutions of IL-8 with increasing concentrations ranging from 1 pg mL^{-1} to 1000 pg mL^{-1}. Fig. 6 illustrates the response of the MWCNTs based immunosensor towards increasing concentrations of IL-8 in the artificial commercialised plasma diluted 1000 times.

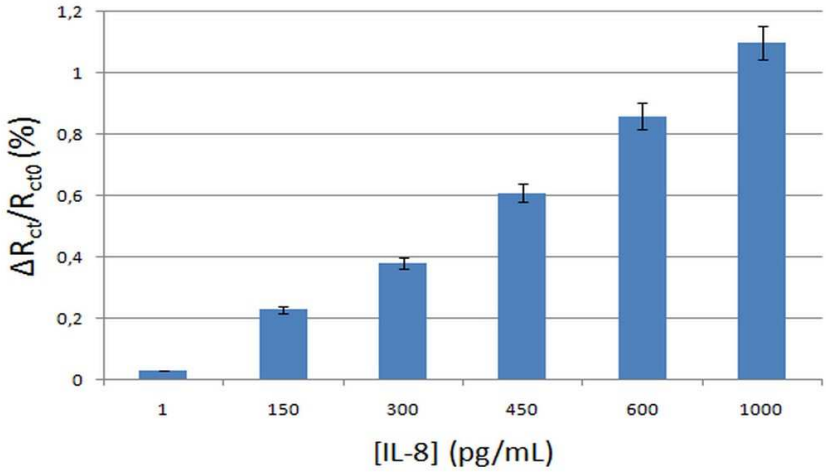

Fig. 6. MWCNTs based immunosensor response towards increasing concentrations of IL-8 in the artificial commercialised plasma diluted 1000 times.

We can observe a considerable dependence of the normalised signal of the developed immunosensor as a function of the IL-8 concentration. Then, in order to prove the absence of non-specific adsorption when detecting IL-8 antigen, we have investigated the response of the sensor towards IL-1 and IL-6 as blank tests. The impedimetric response of aminothiol/ activated MWCNT/ anti IL-8 based immunosensor towards the interfering compounds presented a shift between the two first half-circles. This could be due to the adsorption of proteins found in commercialised artificial plasma. Then, the response of the MWCNTs based nano-architecture was almost the same regardless the increasing concentrations of IL-1 and IL-6. This brings out the high sensitivity and specificity of the developed three-dimensional based impedimetric immunosensor towards IL-8 antigen in artificial plasma, which suggests the possibility of using it in routine procedures for real time monitoring, diagnostic and prognostic of tumor development and progression.

To highlight the advantage of our promising results, Table 4 reports linear concentration ranges and LoDs obtained from other biosensors developed for IL-8 quantification in blood (plasma and serum) by binding with an antibody immobilized onto the working electrode. Compared to them, our device stated lower LoD and wider linear range in addition to a rapid time-analysis and higher selectivity. Moreover, our biosensor resulted more competitive even if compared to the gold standard assays (ELISAs) for IL-8 quantification in blood (plasma and serum), since these assays require longer analysis times (from 4 up to 7 hours), trained personnel and sophisticated equipment, and most of these commercially available IL-8 ELISA kits have proven LoDs of about 15 ± 5 pg mL^{-1}, thus higher than our and above the IL-8 basal clinical level of 5 – 10 pg mL^{-1} commonly detected in healthy patients [25].

Table 2. Comparison of different antibody-based electrochemical immunosensors for IL-8 detection in blood (plasma and serum). Abbreviations: Au: gold; LOD: limit of detection; Ab: antibody; cys: cysteine; C_{60}: spherical fullerenes; ASV: anodic stripping voltammetry; LSV: linear sweep voltammetry; Ti: titanium; TNT: titanium dioxide nanotube.

Transducer	Sensing (Technique)	Linear range	LOD (matrix)	Reference
Carbon electrode	C_{60}/ Ab (ASV/ LSV)	1.25 – 5 ng mL^{-1}	0.61 ± 0.05 ng mL^{-1} (buffer)	[26]
	MWCNTs/Ab (ASV/ LSV)	5 – 20 ng mL^{-1}	0.39 ± 0.10 ng mL^{-1} (buffer)	
Ti electrode	Ti/TNT/Ab (EIS)	5 – 2500 pg mL^{-1}	5 pg mL^{-1} (PBS)	[52]
Au electrode	Aminothiol/Ab (EIS)	150 – 600 pg mL^{-1}	100 pg mL^{-1} (artificial human plasma)	This work
	Aminothiol/ MWCNTs/Ab (EIS)	1 – 1000 pg mL^{-1}	0.1 pg mL^{-1} (artificial human plasma)	

4. Conclusions

In this study, two different spatially hierarchical nano-architectures for real time detection of Interleukin-8 cancer biomarker were developed. A two-dimensional based platform was established by immobilising the activated anti IL-8 onto the aminothiol modified working gold electrode. Then, the integration of MWCNTs, in the functionalisation process, allowed to create a three-dimensional nano-architecture. The electronic properties of MWCNTs and specially their band structure, in terms of density of electronic states, were very important for the interfacial electron transfer between the electroactive species in solution and the working electrode surface. Thus, the use of MWCNTs based three-dimensional nano-architecture leads to the development of a successful and reproducible IL-8 cancer biomarker sensor by improving the immunosensor performances with a low limit of detection and a large linear sensitive range covering the entire clinically interesting range of IL-8 concentrations which is very important not only for the early-stage diagnosis and screening procedures, but also in mapping the stage of the cancer too. Moreover, this device would also represent a promising starting point for further future applications, including its use for saliva analysis, opening the possibility of non-invasive and non-stressful approach to cancer management.

CRediT author statement

Sawsen Azzouzi: Experimental research, Investigation, Writing- Original draft preparation. Mounir Ben Ali: Conceptualization, Methodology, Formal analysis, Supervision, Project administration. Francesca G. Bellagambi: Formal analysis, Reviewing and Editing. Abdelhamid Elaissari: Validation, Editing, Project administration. Nicole Jaffrezic-Renault: Conceptualization, Methodology, Validation, Editing. Abdelhamid Errachid: Conceptualization, Methodology, Supervision, Funding acquisition, Project administration. Nadia Zine: Conceptualization, Methodology, Supervision, Funding acquisition, Project administration.

Declaration of competing interest

The authors declare that they have no known competing financial interests or personal relationships that could have appeared to influence the work reported in this paper.

Acknowledgements

This work was partially supported by the H2020 projects KardiaTool (Grant No. 768686) and WIDESPREAD project (Grant No. 951887), and by POC4Allergies project funded within the ERA PerMed – 2nd Joint Transnational Call for proposals.

References

[1] P. Kuppusamy, N. Govindan, M.M. Yusoff, S.J.A.Ichwan, Proteins are potent biomarkers to detect colon cancer progression, Saudi J. Biol. Sci. 24 (2017):1212–1221. https://doi.org/10.1016/j.sjbs.2014.09.017.

[2] R. Gasparri, G. Sedda, L. Spaggiari, Biomarkers in early diagnosis and early stage lung cancer: The clinician's point of view, J. Clin. Med. 9 (2020) 1790. https://doi.org/doi:10.3390/jcm9061790.

[3] U. Landegren, M. Hammond, Cancer diagnostics based on plasma protein biomarkers: hard times but great expectations, Mol. Oncol. 15 (2021) 1715–1726. https://doi.org/10.1002/1878-0261.12809.

[4] N.C. Japp, J.J. Souchek, A.R. Sasson, M.A. Hollingsworth, S.K. Batra, W.M. Junker, Tumor biomarker in-solution quantification, standard production, and multiplex detection, J. Immunol. Res. 2021 (2021) 9942605. https://doi.org/10.1155/2021/9942605.

[5] E. Dama, T. Colangelo, E. Fina, M. Cremonesi, M. Kallikourdis, G. Veronesi, F. Bianchi, Biomarkers and lung cancer early detection: State of the art, Cancers. 13 (2021) 3919. https://doi.org/10.3390/cancers13153919.

[6] S. Aitekenov, A. Gaipov, R. Bukasov, Review: Detection and quantification of proteins in human urine, Talanta. 223 (2021) 121718. https://doi.org/10.1016/j.talanta.2020.121718.

[7] R. Bhawal, A.L. Oberg, S. Zhang, M. Kohli, Challenges and opportunities in clinical applications of blood-based proteomics in cancer, Cancers (Basel). 12 (2020) 2428. https://doi.org/10.3390/cancers12092428.

[8] D. Vozgirdaite, H. Ben Halima, F.G. Bellagambi, A. Alcacer, F. Palacio, N. Jaffrezic-Renault, N. Zine, J. Bausells, A. Elaissari, A. Errachid, Development of an ImmunoFET for analysis of tumour necrosis factor-α in artificial saliva: Application for heart failure monitoring, Chemosensors. 9 (2021) 26. https://doi.org/10.3390/chemosensors9020026.

[9] H. Ben Halima, F.G. Bellagambi , A. Alcacer, N. Pfeiffer, A. Heuberger, A. Hangouët, N. Zine, J. Bausells, A. Elaissari, A. Errachid, A silicon nitride ISFET based immunosensor for tumor necrosis factor-alpha detection in saliva. A promising tool for heart failure monitoring, Anal. Chim. Acta 1161 (2021) 338468. https://doi.org/10.1016/j.aca.2021.338468.

[10] J.A. Stenken, A.J. Poschenrieder, Bioanalytical chemistry of cytokines--a review, Anal. Chim. Acta. 853 (2015) 95–115. https://doi.org/10.1016/j.aca.2014.10.009.

[11] A.S. Gokhale, R.I. Haddad, L.A. Cavacini, L. Wirth, L. Weeks, M. Hallar, J. Faucher, M.R. Posner, Serum concentrations of interleukin-8, vascular endothelial growth factor, and epidermal growth factor receptor in patients with squamous cell cancer of the head and neck, Oral Oncol. 41 (2005) 70–76. https://doi.org/10.1016/j.oraloncology.2004.06.005.

[12] T.P. Kobawala, G.H. Patel, D.R. Gajjar, K.N. Patel, P.B. Thakor, U.B. Parekh, K.M. Patel, S.N. Shukla, P.M. Shah, Clinical utility of serum interleukin-8 and interferon-alpha in thyroid diseases, J. Thyroid Res. 2011 (2011) 270149. https://doi.org/10.4061/2011/270149.

[13] M. Gonzalez-Aparicio, C. Alfaro, Significance of the IL-8 pathway for immunotherapy, Hum. Vaccin. Immunother. 16 (2020) 2312–2317. https://doi.org/10.1080/21645515.2019.

[14] R. Aalinkeel, M. P.R. Nair, G. Sufrin, S. D. Mahajan, K. C. Chadha, R. P. Chawda, S. A. Schwartz, Cancer Reaserach 64 (2009) 5311–5321.

[15] V. Merz, C. Zecchetto, R. Santoro, F. Simionato, F. Sabbadini, D. Mangiameli, G. Piro, A. Cavaliere, M. Deiana, M.T. Valenti, D. Bazan, V. Fedele, S. Lonardi, D. Melisi, Plasma IL8 Is a Biomarker for TAK1 Activation and Predicts Resistance to Nanoliposomal Irinotecan in Patients with Gemcitabine-Refractory Pancreatic Cancer, Clin Cancer Res 26 (2020) 4661 4669. https://doi.org/10.1158/1078-0432.CCR-20-0395.

[16] C. Alfaro, M.F. Sanmamed, M.E. Rodríguez-Ruiz, Á. Teijeira, C. Oñate, Á. González, M. Ponz, K.A. Schalper, J.L. Pérez-Gracia, I. Melero, Interleukin-8 in cancer pathogenesis, treatment and follow-up, Cancer Treat. Rev. 60 (2017) 24–31. https://doi.org/10.1016/j.ctrv.2017.08.004.

[17] Z. Bakouny, T.K. Choueiri, IL-8 and cancer prognosis on immunotherapy, Nat. Med. 26 (2020) 650–651. https://doi.org/10.1038/s41591-020-0873-9.

[18] B.A. Otieno, C.E. Krause, A. Latus, B.V. Chikkaveeraiah, R.C. Faria, J.F. Rusling, On-line Protein Capture on Magnetic Beads for Ultrasensitive Microfluidic Immunoassays of Cancer Biomarkers, Biosens. Bioelectron. 53 (2014) 268–274. https://doi.org/10.1016/j.bios.2013.09.054.

[19] P. Domnanich, D.B. Pena, C. Preininger, Xanthan/chitosan gold chip for metal enhanced protein biomarker detection, Biosens. Bioelectron. 26 (2011) 2559–2565. https://doi.org/10.1016/j.bios.2010.11.006.

[20] P.S. Waggonera, C.P. Tanb, H.G. Craighead, Microfluidic integration of nanomechanical resonators for protein analysis in serum, Sens. Actuators B-Chem. 150 (2010) 550–555. https://doi.org/10.1016/j.snb.2010.08.041.

[21] R. Malhotra, V. Patel, B.V. Chikkaveeraiah, B.S. Munge, S.C. Cheong, R.B. Zain, M.T. Abraham, D.K. Dey, J.S. Gutkind, J. F. Rusling, Ultrasensitive detection of cancer biomarkers in the clinic by use of a nanostructured microfluidic array, Anal. Chem. 84 (2012) 6249–6255. https://doi.org/10.1021/ac301392g.

[22] S. Mandal, J.M. Goddard, D. Erickson, A multiplexed optofluidic biomolecular sensor for low mass detection, Lab. Chip. 9 (2009) 2924–2932. https://doi.org/10.1039/b907826f.

[23] M.M.A. Hakim, M. Lombardini, K. Sun, F. Giustiniano, P.L. Roach, D.E. Davies, P.H. Howarth, M.R.R. Planque, H. Morgan, P. Ashburn, Thin film polycrystalline silicon nanowire biosensors, Nano Lett. 12 (2012) 1868–1872. https://doi.org/10.1021/nl2042276.

[24] J.T. Kindt, M.S. Luchansky, J. Abraham, A.J. Qavi, S.H. Lee, R.C. Bailey, Subpicogram per milliliter detection of interleukins using silicon photonic microring resonators and an

enzymatic signal enhancement strategy, Anal. Chem. 85 (2013) 10653−10657. https://doi.org/10.1021/ac402972d.

[25] R. Sharma, S.E. Deacon, D. Nowak, S.E. George, M.P. Szymonik, A. Tang, D.C. Tomlinson, A.G. Davies, M.J. McPherson, C. Wälti, C. (2016). Label-free electrochemical impedance biosensor to detect human interleukin-8 in serum with sub-pg/ml sensitivity. Biosensors & bioelectronics, 80 (2016) 607–613. https://doi.org/10.1016/j.bios.2016.02.028.

[26] S. Tonello, M. Marziano, G. Abate, T. Kilic, M. Memo, D. Uberti, S. Carrara, N.F. Lopomo, M.Serpelloni, E. Sardini, Enhanced sensing of interleukin 8 by stripping voltammetry: Carbon nanotubes versus fullerene, in: Eskola H., Väisänen O., Viik J., Hyttinen J. (eds) EMBEC & NBC 2017. EMBEC 2017, NBC 2017. IFMBE Proceedings, vol 65. Springer, Singapore, 2018, pp. 213–216. https://doi.org/10.1007/978-981-10-5122-7_54.

[27] J. Verbarg, O. Hadass, P.D. Olivo, A. Danielli, High sensitivity detection of a protein biomarker interleukin-8 utilizing a magnetic modulation biosensing system, Sens. Actuators B-Chem. 241 (2017) 614–618. https://doi.org/10.1016/j.snb.2016.10.089.

[28] J. Bausells, H. Ben Halima, F.G. Bellagambi, A. Alcacer, N. Pfeiffer, M. Hangouët, N. Zine, A. Errachid, On the impedance spectroscopy of field-effect biosensors, Electrochem. Sci. Adv. 2021 (2021) e2100138. https://doi.org/ doi.org/10.1002/elsa.202100138.

[29] B. V. Chikkaveeraiah, A. A. Bhirde, N. Y. Morgan, H. S. Eden, X. Chen, Electrochemical Immunosensors for Detection of Cancer Protein Biomarkers, ACS Nano 6 (2012) 6546–6561. https://doi.org/ 10.1021/nn3023969.

[30] C. Paoletti, M. He, P. Salvo, B. Melai, N. Calisi, M. Mannini, B. Cortigiani, F.G. Bellagambi, T.M. Swager, F. Di Francesco, A. Pucci, Room temperature amine sensors enabled by sidewall functionalization of single-walled carbon nanotubes, RSC Adv. 8 (2018) 5578−5585. https://doi.org/10.1039/C7RA13304A.

[31] M. Nurazzi Norizan, M.H. Moklis, S.Z. Ngah Demon, N.A. Halim, A. Samsuri, I.S. Mohamad, V.F. Knight, N. Abdullah, Carbon nanotubes: functionalisation and their application in chemical sensors, RSC Adv. 10 (2020) 43704–43732. https://doi.org/10.1039/D0RA09438B.

[32] N.G. Welch, J.A. Scoble, B.W. Muir, P.J. Pigram, Orientation and characterization of immobilized antibodies for improved immunoassays (Review), Biointerphases. 12 (2017) 02D301. https://doi.org/10.1116/1.4978435.

[33] S. Chen, L. Liu, J. Zhou, S. Jiang, Controlling Antibody Orientation on Charged Self-Assembled Monolayers, Langmuir. 19 (2003) 2859–2864. https://doi.org/10.1021/la026498v.

[34] A. Baraket, M. Lee, N. Zine, N. Yaakoubi, M.G. Trivella, A. Elaissari, M. Sigaud, N. Jaffrezic-Renault , A. Errachid, A flexible label-free biosensor sensitive and selective to TNF-α: application for chronic heart failure, Sens. Transducers. 27 (2014), 15–21.

[35] E. Venturelli, C. Fabbro, O. Chaloin, C. Ménard-Moyon, C.R. Smulski, T. Da Ros, K. Kostarelos, M. Prato, A. Bianco, Antibody covalent immobilization on carbon nanotubes and assessment of antigen binding, Small. 7 (2011) 2179–2187. https://doi.org/10.1002/smll.201100137.

[36] M. Ben Ali, F. Bessueille, J.M. Chovelon, A. Abdelghani, N. Jaffrezic-Renault, M.A. Maaref, C. Martelet, Use of ultra-thin organic silane films for the improvement of gold adhesion to the silicon dioxide wafers for (bio)sensor applications, Mater. Sci. Eng. C 28 (2008) 628–632. https://doi.org/10.1016/j.msec.2007.10.048.

[37] N.S. Ferreira, M.G.F. Sales, Disposable immunosensor using a simple method for oriented antibody immobilization for label-free real-time detection of an oxidative stress biomarker implicated in cancer diseases, Biosens. Bioelectron. 53 (2014) 193–199. https://doi.org/10.1016/j.bios.2013.09.056.

[38] S. Bourigua, A. Maaref, A. Errachid, F. Bessueille, N. Jaffrezic-Renault, Immunosensors based on single-walled carbon nanotubes (SWCNT) for the detection of deep venous thrombosis, Sens. Transducers. 27 (2014) 127–136.

[39] S. Bourigua, M. Hnaien, F. Bessueille, F. Lagarde, S. Dzyadevych, A. Maaref, J. Bausells, A. Errachid, N. Jaffrezic Renault, Impedimetric immunosensor based on SWCNT-COOH modified gold microelectrodes for label-free detection of deep venous thrombosis biomarker, Biosens Bioelectron. 26 (2010) 1278–1282. https://doi.org/10.1016/j.bios.2010.07.004.

[40] F.G. Bellagambi, A. Baraket, A. Longo, M. Vatteroni, N. Zine, J. Bausells, R. Fuoco, F. Di Francesco, G.S. Karanasiou, D.I. Fotiadis, A. Menciassi, A.Errachid, Electrochemical biosensor platform for TNF-α cytokines detection in both artificial and real human saliva: Heart failure, Sens. Actuators B Chem. 251 (2017) 1026–1033. https://doi.org/10.1016/j.snb.2017.05.169.

[41] L. Barhoumi, A. Baraket, F.G. Bellagambi, G.S. Karanasiou, M. Ben Ali, D.I. Fotiadis, J. Bausells, N. Zine, M. Sigaud, A. Errachid, A novel chronoamperometric immunosensor

667 for recombinant human TNF-α detection. Sens. Actuators B Chem. 266 (2018) 477–484.
668 https://doi.org/10.1016/j.snb.2018.03.135.
669 [42] L. Barhoumi, F.G. Bellagambi, F.M. Vivaldi, A. Baraket, Y. Clément, N. Zine, M. Ben
670 Ali, A. Elaissari, A. Errachid, Ultrasensitive immunosensor array for TNF-α detection in
671 artificial saliva using polymer-coated magnetic microparticles onto screen-printed gold
672 electrode, Sensors. (Basel.) 19 (2019) 692. https://doi.org/10.3390/s19030692.
673 [43] M. Hnaien, S. Bourigu, F. Bessueille, J. Bausells, A. Errachid, F. Lagard, N. Jaffrezic-
674 Renault, Impedimetric microbial biosensor based on single wall carbon nanotube
675 modified microelectrodes for trichloroethylene detection, Electrochim. Acta 56 (2011)
676 10353–10358. https://doi.org/10.1016/j.electacta.2011.04.041.
677 [44] M. Ben Ali, Y. Korpan, M.A. Gonchar, El'skaya, M.A. Maaref, , N. Jaffrezic-Renault, C.
678 Martelet, Formaldehyde assay by capacitance versus voltage and impedance
679 measurements using bi-layer bio-recognition membrane, Biosens. Bioelectron. 22 (2006)
680 575–581. https://doi.org/10.1016/j.bios.2006.01.019.
681 [45] M. Barreiros dos Santos, J.P. Agusil, B. Prieto-Simon, C. Sporer, V. Teixeira, J.
682 Samitier, Highly sensitive detection of pathogen Escherichia coli O157:H7 by
683 electrochemical impedance spectroscopy, Biosens. Bioelectron. 45 (2013) 174–180.
684 https://doi.org/10.1016/j.bios.2013.01.009.
685 [46] N. J. Ronkainen, H.B. Halsall, W.R. Heineman, Electrochemical biosensors, Chem. Soc.
686 Rev. 39 (2010) 1747–1763. https://doi.org/10.1039/b714449k.
687 [47] L.G. Zamfir, I. Geana,1, S. Bourigua, L. Rotariu, C. Bala, A. Errachid, N. Jaffrezic-
688 Renault, Highly sensitive label-free immunosensor for ochratoxin A based on
689 functionalized magnetic nanoparticles and EIS/SPR detection, Sens. Actuators B Chem.
690 159 (2011) 178– 184. https://doi.org/10.1016/j.snb.2011.06.069.
691 [48] M. Lee, N. Zine, A. Baraket, M. Zabala, F. Campabadal, R. Caruso, M.G. Trivella, N.
692 Jaffrezic-Renault, A. Errachid, A novel biosensor based on hafnium oxide: Application
693 for early stage detection of human interleukin-10, Sens. Actuators B Chem. 175 (2012)
694 201– 207. https://doi.org/10.1016/j.snb.2012.04.090.
695 [49] A. Baraket, M. Lee, N. Zine, M. Sigaud, N. Yaakoubi, M. G. Trivella, M. Zabala, J.
696 Bausells, N. Jaffrezic-Renault, A. Errachid, Diazonium modified gold microelectrodes
697 onto polyimide substrates for impedimetric cytokine detection with an integrated
698 Ag/AgCl reference electrode, Sens. Actuators B Chem. 189 (2013) 165–172.
699 https://doi.org/10.1016/j.snb.2013.02.088.

[50] V. Gelfo, D. Romaniello, M. Mazzeschi, M. Sgarzi, G. Grilli, A. Morselli, B. Manzan, K. Rihawi, M. Lauriola, Roles of IL-1 in cancer: From tumor progression to resistance to targeted therapies, Int. J. Mol. Sci. 21 (2020) 6009. https://doi.org/10.3390/ijms21176009.

[51] T. Hirano, IL-6 in inflammation, autoimmunity and cancer, Int. Immunol. 33 (2021) 127–148. https://doi.org/10.1093/intimm/dxaa078.

[52] K. Arkusz, E. Paradowska, Impedimetric Detection of femtomolar levels of Interleukin6, Interleukin 8, and Tumor Necrosis Factor Alpha based on thermally modified nanotubular titanium dioxide arrays, Nanomaterials (Basel). 10 (2020) 2399. https://doi.org/10.3390/nano10122399.